Magnetic Exchange Splitting in Fe above the Curie Temperature

M. Pickel,[1,2] A. B. Schmidt,[2,1] M. Weinelt,[2,3] and M. Donath[1,*]

[1]*Physikalisches Institut, Westfälische Wilhelms–Universität Münster, Wilhelm-Klemm-Straße 10, 48149 Münster, Germany*

[2]*Max-Born-Institut, Max-Born-Straße 2A, 12489 Berlin, Germany*

[3]*Freie Universität Berlin, Fachbereich Physik, Arnimallee 14, 14195 Berlin, Germany*

(Received 18 December 2009; revised manuscript received 3 February 2010; published 9 June 2010)

The magnetic exchange splitting of electronic states in a 7 monolayer Fe film on Cu(001) was investigated below and above the Curie temperature T_C, using image-potential surface states as sensor. At T_C, the long-range magnetic order breaks down as reflected by a vanishing spin splitting and vanishing spin polarization. The exchange splitting, in contrast, does not change abruptly at T_C but persists up to $T = 1.2T_C$. Equally, the spin-integrated linewidth shows no signature of the magnetic phase transition but smoothly decreases with increasing temperature. Our experimental results confirm theoretical expectations that, at T_C, the long-range magnetic order disappears but the local magnetic moments and, in particular, the valence electronic structure are unaffected by the phase transition.

DOI: 10.1103/PhysRevLett.104.237204 PACS numbers: 75.40.−s, 73.20.At, 75.70.Ak, 79.60.Dp

The question of how the magnetic phase transition is reflected in the electronic structure has been addressed by several experimental studies but never answered unequivocally. The magnetic ground state is considered as characterized by mainly pure spin states, separated in energy for majority and minority spin by the exchange splitting. This splitting depends on the band character, the wave vector, the energy, and possibly the temperature. With increasing temperature, the magnetization is lowered until the long-range magnetic order is lost at the Curie temperature T_C. Does the exchange splitting collapse at T_C or do the spin states mix? Neutron and electron-energy-loss experiments found evidence of local magnetic moments above T_C [1,2]. Photoemission, inverse-photoemission, and scanning tunneling spectroscopy experiments give confusing or even conflicting pictures of collapsing, spin-mixing, or intermediate band behavior for the $3d/4s$ valence bands in Fe [3–5], Ni [6–14], and Co [15], and for the $5d/6s$ bands in Gd [16–23]. A number of theoretical investigations modeled the magnetic finite-temperature behavior with different approaches, e.g., local-band theory, disordered-local-moment model, many-body theory, spin-fluctuation theory, dynamical mean-field theory [24–30].

Unfortunately, the discriminatory power of most experiments with respect to the theoretical models is rather limited. First, it is difficult to disentangle magnetic from phonon-induced changes, because usually measurements of the electronic structure suffer from temperature-induced linewidth broadening due to phonons. This is especially true for exchange splittings that are in the order of the linewidths. Additionally, the analysis is usually complicated by nonlinear and spin-dependent background intensities. Second, the loss of long-range magnetic order above T_C leads to vanishing magnetic or spin contrast in experiments. Therefore, most of the electronic-structural data stop at or a little above T_C, thus failing to investigate possible changes well above T_C.

In this Letter we present data of the Fe valence electronic structure for temperatures below and well above T_C. We show that the use of image-potential states [31] as sensor states opens the way to study magnetic effects in the electronic structure, yet decoupled from phonons. By using polarization-dependent and spin-resolved two-photon photoemission (2PPE), we are able to follow the exchange splitting upon crossing T_C in the relevant temperature range up to $1.2T_C$ in background-free spectra. Moreover, no external fields are necessary during our measurements, unlike in other approaches, such as susceptibility measurements via magneto-optical Kerr effect. As the susceptibility diverges at T_C, already weak external magnetic fields may cause spurious magnetic response.

As a test case, we investigated 7 monolayer (ML) Fe films on Cu(001) grown at room temperature by thermal deposition. With 270 K, this system has a T_C that is easily accessible in the experiment. The two outermost atomic layers of the Fe film are ferromagnetic with out-of-plane anisotropy [32], whereas the magnetic structure of the Fe layers underneath can be described by a spin-density wave with a Néel temperature T_N of about 200 K [33]. Hence, for temperatures above T_N and below T_C, a quasi-two-dimensional ferromagnetic Fe film exists on a paramagnetic underlayer [34,35].

In our 2PPE experiment, the frequency-tripled femtosecond laser pulses from a Ti:sapphire oscillator (photon energy $\hbar\omega_a = 4.68$ eV) are used as pump pulses to populate the image-potential states from states below the Fermi energy E_F (schematically shown in Fig. 1). A second laser pulse (photon energy $\hbar\omega_b = 1.56$ eV) excites the electrons above the vacuum level E_{vac}. The photoelectrons are then detected with a 90° electrostatic analyzer with an energy

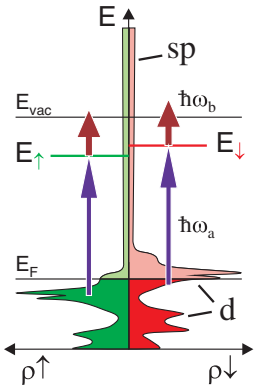

FIG. 1 (color online). Schematic energy diagram of a spin-dependent two-photon-photoemission process at a ferromagnetic metal. Electrons are excited via ultraviolet pump pulses ($\hbar\omega_a$) from spin-dependent occupied states into exchange-split image-potential states ($E_\uparrow$ and $E_\downarrow$) which serve as intermediate states. Their population depends on matrix-element effects associated with the excitation process from the initial states. This leads to a spin-dependent population of the image-potential states. Infrared laser pulses ($\hbar\omega_b$) probe population and temperature-dependent energy of these states by exciting them above the vacuum energy E_{vac}.

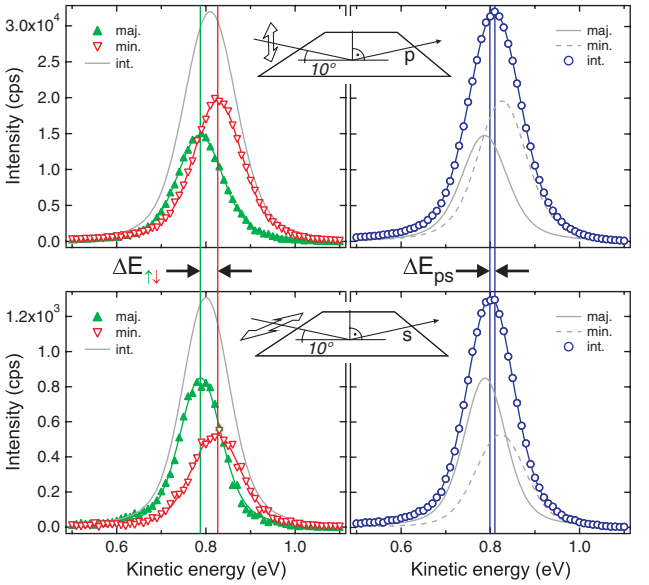

FIG. 2 (color online). Two-photon-photoemission spectra of 7 ML Fe on Cu(001) obtained with p-polarized (upper panel) and s-polarized (lower panel) pump light ($\hbar\omega_a = 4.43$ eV) at a sample temperature of $T = 252$ K. The spin-resolved spectra in the left-hand panels reveal the spin splitting $\Delta E_{\uparrow\downarrow}$, while the spin-integrated spectra in the right-hand panels show the energy shift ΔE_{ps} between the spectra obtained with p- and s-polarized pump light.

resolution of 65 meV. The spin resolution was provided by a spin-polarization detector based on SPLEED (spin-polarized low-energy electron diffraction) [36,37] with a Sherman function of 0.24 ± 0.02. The sample was remanently magnetized during the measurements. Data were obtained for both magnetization directions to prevent experimental artifacts in the spin analysis. Further information about experimental setup and sample preparation is published elsewhere [38].

In this study, we combine polarization-dependent and spin-resolved 2PPE to extract the magnetic exchange splitting below and above T_C. In a ferromagnet (below T_C), the electronic states are exchange split; i.e., they have spin-dependent binding energies, which entails the following. First, we expect a spin-dependent density of states at the initial-state energy, which lies $\hbar\omega_a$ below the image-state energy (cf. Fig. 1). In the photoexcitation process, the spin is conserved and the spin-dependent density of states is projected onto the image states [39]. This is the reason for the spin-dependent population of image states, which results in spin-dependent intensities (spin polarization) of image states as observed in the left-hand panels of Fig. 2. As the strength of an optical excitation is not only determined by the density of states, but also governed by dipole-selection rules, we find different spin polarizations for different excitation symmetries (upper and lower panel of Fig. 2): With p-polarized pump pulses, dipole transitions occur mainly from sp bands, while s-polarized light excites the d electrons into the image-potential states [40]. The spin-dependent 2PPE intensities are, therefore, an effect of the spin polarization of the initial bulk states. Second, the image states are exchange split because they mirror the spin-dependent bulk-band-gap boundaries [41,42]. This appears in the spin-resolved spectra as a spin splitting $\Delta E_{\uparrow\downarrow}$ between spin-up and spin-down spectral features.

The combination of spin-dependent intensities depending on the light polarization and spin-dependent binding energies leads to a distinct peak position in the spin-integrated spectrum. The maximum of this peak shifts towards the minority-spin image-state energy for excitation with p-polarized light and towards the majority-spin image-state energy for s-polarized light (right-hand panels of Fig. 2). We will call this shift of the energetic position ΔE_{ps}. In order to observe a nonzero ΔE_{ps} in the spin-integrated spectrum, two conditions have to be met: (i) the initial states have to be spin dependent and (ii) the image states have to be exchange split. The size of ΔE_{ps} depends in a nontrivial way on the exchange splitting of image states and the matrix elements associated with the excitation process. The excitation energy $\hbar\omega_a$ and the image-state energies $E_\uparrow$ and $E_\downarrow$ determine the initial-state energies from which the excitations occur (cf. Fig. 1). In combination with dipole-selection rules, this generally leads to different spin-dependent populations of the image states. In our case shown in Fig. 2, more minority electrons are excited with p-polarized light, while more majority electrons are excited with s-polarized light. This leads to a ΔE_{ps} of about 10 meV below T_C. ΔE_{ps} can be optimized

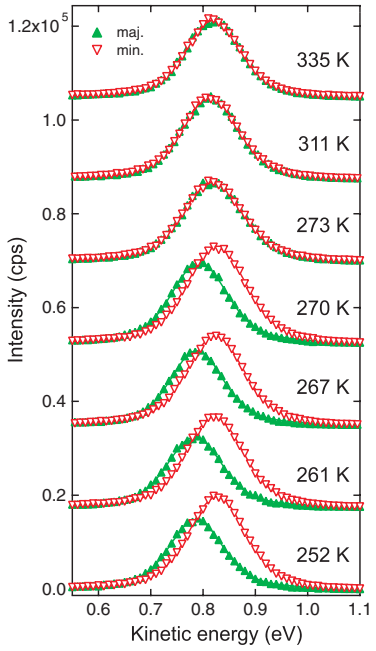

FIG. 3 (color online). Temperature dependence of spin-resolved two-photon-photoemission spectra for 7 ML Fe on Cu(001). The pump pulses for these measurements were p polarized with a photon energy of $\hbar\omega_a = 4.43$ eV.

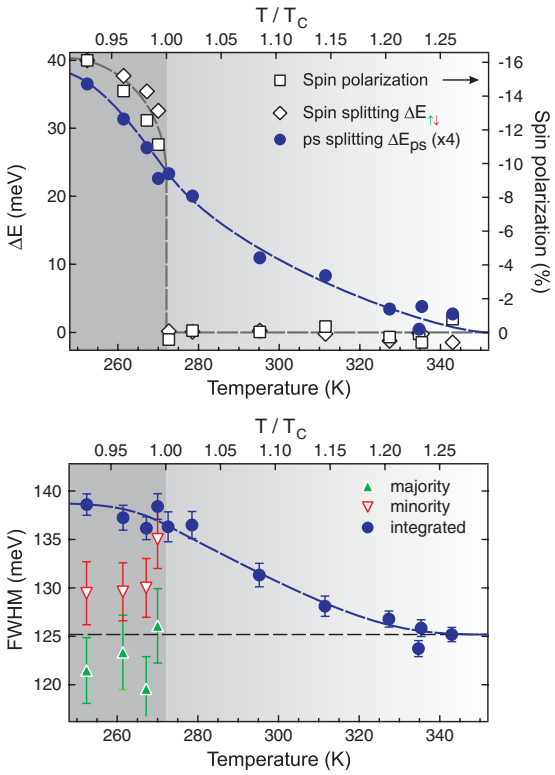

FIG. 4 (color online). Spin polarization, spin splitting $\Delta E_{\uparrow\downarrow}$, and ps splitting ΔE_{ps} of the $n = 1$ image-potential state for 7 ML Fe on Cu(001) as a function of temperature (upper panel, error bars are within the symbol size). Spin-dependent and spin-integrated image-potential-state linewidths (for p-polarized pump pulse) as a function of temperature (lower panel). The dashed lines in both panels are guides to the eye.

by tuning the excitation energy but cannot be directly translated to, e.g., the magnetic moment. We have thus established ΔE_{ps} as a direct consequence of both spin-dependent initial states and exchange-split image states. This promises unique experimental access to any spin dependence of the local electronic structure, even above T_C.

Here, the loss of long-range magnetic order leads to vanishing magnetic or spin contrast in, e.g., Kerr measurements or electron spectroscopies, just as we observe. Figure 3 shows spin-resolved 2PPE spectra of the $n = 1$ image-potential state at 7 ML Fe/Cu(001) for p-polarized pump pulses at temperatures between 252 and 335 K. For $T \approx 252$ K, the image state shows a clear splitting of 40 meV combined with spin-dependent intensities as a consequence of the excitation process. For temperatures higher than T_C, the spin dependence in the 2PPE signal disappears: both spin splitting and spin polarization collapse as shown in the upper panel of Fig. 4. The collapse is a direct consequence of the loss of long-range magnetic order at T_C. However, ΔE_{ps} shows a monotonic decrease with no sign of the phase transition. The finite ΔE_{ps} above T_C proves the spin dependence of both initial states and image states well above the magnetic phase transition up to $T/T_C = 1.2$. This result tells us that the local electronic structure involved in the optical transitions keeps a finite exchange splitting well above T_C, which in turn gives evidence of local magnetic moments. In our specific two-dimensional magnetic system, the local exchange splitting persists up to about 50 K above T_C.

As already mentioned, conclusions with respect to a spin-mixing or Stoner-like scenario are usually hindered by temperature-induced linewidth broadening of the spectral features, which cannot be separated unambiguously from magnetic effects [9]. This is not the case here, because image states are almost decoupled from phonons due to the small overlap between image-state and bulk-state wave functions [43,44]. In the lower panel of Fig. 4, the spin-resolved and spin-integrated linewidths of the $n = 1$ image states are displayed as a function of the temperature. For temperatures below T_C, the linewidth for minority spin is larger than for majority spin. This is a direct consequence of spin-dependent decay channels [45,46]. The striking result is that the spin-integrated linewidth does not increase with increasing temperature, as would be expected for a phonon-induced effect, but clearly decreases. Therefore, this drop of the linewidth must be magnetically induced. We know from the nonzero ΔE_{ps} above T_C that the image states are still exchange split. The reduced linewidth can therefore be understood as a consequence of a merging exchange splitting above T_C. This observation agrees with the observed decrease of ΔE_{ps}. Both results point to a decreasing exchange splitting with

increasing temperature. However, there is no collapse of the exchange splitting at T_C. The data of Fig. 4 show that the temperature dependence of the local exchange splitting does not reflect the magnetic phase transition.

While the spin polarization and the spin splitting unsurprisingly vanish at the Curie temperature, ΔE_{ps} is not affected by the breakdown of the macroscopic magnetization, i.e., the long-range magnetic order. This is only possible if a local exchange splitting of both the sp and d bulk bands and the image-potential states is still present for several tens of kelvin above T_C. As the lateral extension of the image-potential state is of the order of 50 Å [47], i.e., much more than one lattice constant, short-range magnetic order must still be present on this length scale at least. Where techniques which average over larger areas will show no magnetic contrast, ΔE_{ps} will persist as long as a local exchange splitting exists and the order length scale is larger than the image-potential-state wave function. Furthermore, possible temporal fluctuations of the local magnetic moment must be slower than the time resolution of the 2PPE experiment of 70 fs. A breakup into microdomains usually shows up as a loss of macroscopic magnetization in any spatially integrating experiment, e.g., above T_C or after ultrafast laser excitation. However, via ΔE_{ps}, the image-potential states provide an additional local probe in an otherwise spatially integrating experiment.

In conclusion, we show that our experimental approach of polarization-dependent and spin-resolved two-photon photoemission provides unbiased, i.e., zero-field, access to the band structure at the magnetic phase transition below and above the Curie temperature. The use of image-potential states as sensors allowed us to study temperature-dependent magnetic effects decoupled from phonon-induced temperature broadening. Our observation of a finite ΔE_{ps} up to 50 K above the Curie temperature is a clear sign of local magnetic order persisting well above T_C with the lateral extension of our sensor states providing a lower boundary of some ten angstrom for the size of these microdomains.

Financial support by the Deutsche Forschungsgemeinschaft is gratefully acknowledged.

*markus.donath@uni-muenster.de

[1] H. A. Mook, J. W. Lynn, and R. M. Nicklow, Phys. Rev. Lett. **30**, 556 (1973).
[2] J. Kirschner and E. Langenbach, Solid State Commun. **66**, 761 (1988).
[3] E. Kisker *et al.*, Phys. Rev. Lett. **52**, 2285 (1984).
[4] J. Kirschner *et al.*, Phys. Rev. Lett. **53**, 612 (1984).
[5] E. Kisker *et al.*, Phys. Rev. B **31**, 329 (1985).
[6] H. Hopster *et al.*, Phys. Rev. Lett. **51**, 829 (1983).
[7] M. Donath and V. Dose, Europhys. Lett. **9**, 821 (1989).
[8] K.-P. Kämper, W. Schmitt, and G. Güntherodt, Phys. Rev. B **42**, 10 696 (1990).
[9] J. Würtenberg *et al.*, Phys. Scr. **41**, 634 (1990).
[10] W. von der Linden, M. Donath, and V. Dose, Phys. Rev. Lett. **71**, 899 (1993).
[11] A. Kakizaki *et al.*, Phys. Rev. Lett. **72**, 2781 (1994).
[12] J. Fujii *et al.*, Solid State Commun. **94**, 391 (1995).
[13] P. Aebi *et al.*, Phys. Rev. Lett. **76**, 1150 (1996).
[14] B. Sinkovic *et al.*, Phys. Rev. Lett. **79**, 3510 (1997).
[15] C. M. Schneider *et al.*, Europhys. Lett. **16**, 689 (1991).
[16] Dongqi Li *et al.*, Phys. Rev. B **45**, 7272 (1992).
[17] Bongsoo Kim *et al.*, Phys. Rev. Lett. **68**, 1931 (1992).
[18] A. V. Fedorov, K. Starke, and G. Kaindl, Phys. Rev. B **50**, 2739 (1994).
[19] Dongqi Li *et al.*, Phys. Rev. B **51**, 13 895 (1995).
[20] M. Donath, B. Gubanka, and F. Passek, Phys. Rev. Lett. **77**, 5138 (1996).
[21] E. Weschke *et al.*, Phys. Rev. Lett. **77**, 3415 (1996).
[22] M. Getzlaff *et al.*, J. Magn. Magn. Mater. **184**, 155 (1998).
[23] K. Maiti *et al.*, Phys. Rev. Lett. **88**, 167205 (2002).
[24] V. Korenman and R. E. Prange, Phys. Rev. Lett. **44**, 1291 (1980).
[25] K. Usami and T. Moriya, Solid State Commun. **36**, 619 (1980).
[26] W. Borgieł, W. Nolting, and M. Donath, Solid State Commun. **72**, 825 (1989).
[27] W. Nolting, A. Vega, and Th. Fauster, Z. Phys. B **96**, 357 (1995).
[28] M. Uhl and J. Kübler, Phys. Rev. Lett. **77**, 334 (1996).
[29] A. I. Lichtenstein, M. I. Katsnelson, and G. Kotliar, Phys. Rev. Lett. **87**, 067205 (2001).
[30] C. Santos, W. Nolting, and V. Eyert, Phys. Rev. B **69**, 214412 (2004).
[31] P. M. Echenique *et al.*, Surf. Sci. Rep. **52**, 219 (2004).
[32] J. Thomassen *et al.*, Phys. Rev. Lett. **69**, 3831 (1992).
[33] D. Qian *et al.*, Phys. Rev. Lett. **87**, 227204 (2001).
[34] B. Gubanka, M. Donath, and F. Passek, J. Magn. Magn. Mater. **161**, L11 (1996).
[35] M. Donath *et al.*, J. Phys. Condens. Matter **21**, 134004 (2009).
[36] J. Kirschner and R. Feder, Phys. Rev. Lett. **42**, 1008 (1979).
[37] D. H. Yu *et al.*, Surf. Sci. **601**, 5803 (2007).
[38] M. Weinelt *et al.*, Prog. Surf. Sci. **82**, 388 (2007).
[39] M. Pickel *et al.*, Phys. Rev. Lett. **101**, 066402 (2008).
[40] W. Eberhardt and F. J. Himpsel, Phys. Rev. B **21**, 5572 (1980).
[41] F. J. Himpsel, Phys. Rev. B **43**, 13 394 (1991).
[42] M. Donath *et al.*, Surf. Sci. **601**, 5701 (2007).
[43] E. Knoesel, A. Hotzel, and M. Wolf, J. Electron Spectrosc. Relat. Phenom. **88**, 577 (1998).
[44] M. Weinelt, J. Phys. Condens. Matter **14**, R1099 (2002).
[45] F. Passek *et al.*, Phys. Rev. Lett. **75**, 2746 (1995).
[46] A. B. Schmidt *et al.*, Phys. Rev. Lett. **95**, 107402 (2005).
[47] R. Fischer, Th. Fauster, and W. Steinmann, Phys. Rev. B **48**, 15 496 (1993).